Eleventh South African Conference on Computational and Applied Mechanics
SACAM 2018
Vanderbijlpark, South Africa, 17-19 September 2018

Experimental and Numerical Validation of a Simplified Rigid Torso Surrogate used for Investigating the Fluid-Structure Interaction of Air Blast Waves

Thanyani Pandelani[a,b], Zelldra Schutte[a] and Elsmari Wium[a]

[a]*CSIR Defence, Peace, Safety and Security,1 Meiring Naude Road, Pretoria, 0001, South Africa*

[b]*Department of Bioengineering, Imperial College London, 1 Exhibition Road, London, SW72AZ, United Kingdom*

email address : Tpandelani@csir.co.za[a,b], Zschutte@csir.co.za[a], Ewium@csir.co.za[a]

Abstract

Blast waves from landmines and Improvised Explosive Devices (IEDs) produce an almost instantaneous rise in pressure which causes Primary Blast Injuries (PBI). The primary blast injuries are caused directly by the blast wave and encompasses injury to air containing organs such as the lung, ear, and bowel. The most notable primary injury is the blast lung, which is a contusion of lungs in which blood contaminates the alveoli leading to death. The PBI criteria are specified in test standards to relate pressure measurements in a testing environment to a risk of PBI. This study examines the adequacy of using a torso surrogate to measuring pressure profiles both experimentally and numerically.

A simplified rigid human torso surrogate, referred to as the Blast Test Device (BTD), was manufactured and tested. The BTD comprises a high-density polyethylene (HDPE) cylinder with an outer diameter of 300 mm, height of 802 mm and wall thickness of 20 mm. The BTD was exposed to complex blast waves in free-field conditions, which were created by detonating 300 g Plastic Explosive (PE4) at three different heights above ground over a smooth, concrete surface.

The experimental results were compared to the numerical results as well as results available in literature. The experimental results were compared with respect to incident pressures, reflected pressures and positive phase duration of the blast wave. Morphological correlation was observed between the experimental and literature results, however time delays for initial peaks were observed in three of the comparisons. The numerical predictions also compared well morphologically, but with time delays observed for side-on pressures, as well as differences in initial peak pressures.

Keywords: Fluid-structure interaction; IEDs; primary blast injury, overpressure; injury citeria; Blast Test Device, BTD, torso

1. Introduction

Detonating an explosive charge generates the propagation of a shock-wave, which principally affects gas-containing organs, such as the lungs, the middle ear and gastrointestinal tract [1]. The nature and extent of the resulting injury depend on the type of explosive device used and the environment within which it detonates. The use of improvised explosive devices (IEDs) results in more complex waves, with multiple reflections that can interact simultaneously with the soldier, resulting in more severe injuries. The use of IEDs became the first cause of injuries on the Battlefield, with up to 60 % death on the US forces in Operation Enduring Freedom in Afghanistan [2].

In a free-field environment, the pressure-time history resulting from a detonation has a well-known shape, called the Friedlander profile. Friedlander waveforms are commonly used for blast interaction studies. However, a soldier does not only face idealised shocks. Reflections of the wave on the ground or any obstacles are factors that complicate the pressure-time histories. Simplified rigid and deformable thorax models have been developed to record the pressure at different locations, as well as the motion of those surrogates for blast studies such as a Blast Test Device (BTD) [3].

In the interest of developing equipment that will protect soldiers during IED attacks, it is important to understand the complexity, path and pressure range of the blast waves. In this study, the focus was on blast interaction with simplified torso surrogate called the BTD. A reduce-scaled experiments were preferred to full-scaled experiments because of free-field experimental ground availability. To reproduce scenarios that can be seen on the battlefield, three different scenarios were investigated: a charge close to the ground, a charge at a mid-sternum human height, and finally, an intermediate configuration will be performed. A numerical model was also developed to compare with the experimental results.

1.1. Blast waves

Upon the initiation of an explosive charge, a blast wave is generated due to the rapid expansion of detonation gases [4]. When the blast wave interacts with other structures, such as the ground, a triple point is formed. The triple point occurs when the reflected blast wave from the ground catches the initial incident blast wave, forming an intense shock wave, called the Mach stem. This phenomenon is illustrated in Figure 1.

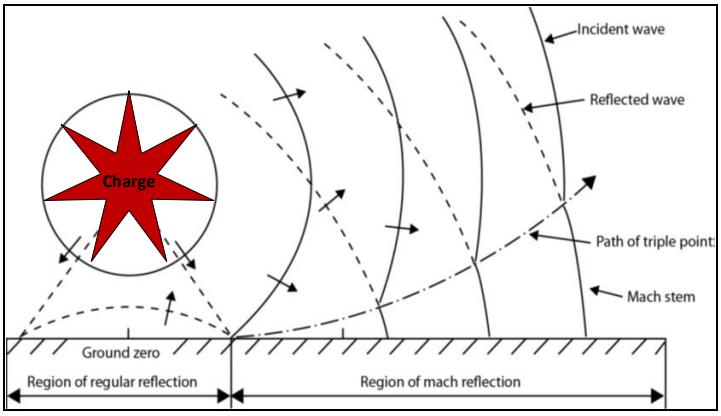

Fig. 1. Schematic of the Mach stem formation and the path of the triple point [5]

To prevent primary blast injuries, it is required to characterise the blast wave profile to quantify the level of injury due to a given blast wave. Blast waves can be classified as either simple blast waves (i.e. free-field, open air blast waves) or complex blast waves (waves interacting with other structures). Each type of blast wave has a distinct blast wave profile [6, 7].

The temporal pressure profile of a simple blast wave is known as the Friedlander waveform in its most ideal form (Figure 2). The Friedlander waveform has an immediate rapid positive pressure, followed by a slower exponential decay, followed by a negative pressure phase duration, before recovering back to the ambient pressure [4, 6 - 9].

In contrast to the simple Friedlander type blast waves, are complex blast waves (Figure 3). Complex waves are any combination of waves reflected from multiple directions producing secondary waves [4, 7]. Most real-world explosions produces complex waves, as waves can be reflected from surroundings like the ground, walls and any other nearby object.

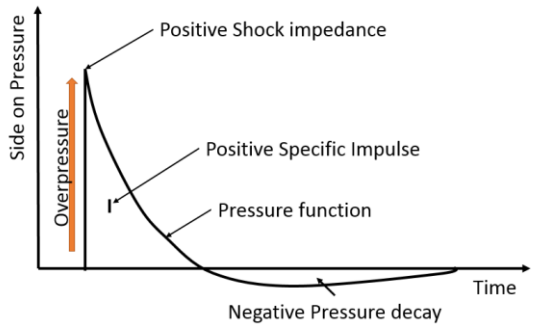

Fig. 2. Friedlander waveform [4, 8]

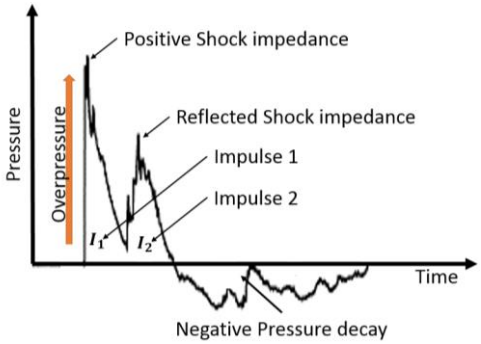

Fig. 3. Complex pressure waveform [4].

1.2. Injury prediction

To measure the effect of pressure profiles on humans, specific injury criteria have been developed. These injury criteria can usually be defined into criteria which measures either the injury severity or injury lethality. Severity criteria usually measure the probability of injuries on a specific scale, whereas lethality usually indicate probability of death in a specific timeframe after impact. Both can be developed either from data obtained from human injuries or by using scaling models from animal, mechanical and frangible surrogates that can relate measurements recorded during an explosive event to a risk of injury to the torso body region.

In the 1960s, Bowen [10] developed scaled lethality curves for a 70 kg man exposed to simple blast wave profiles. The Bowen model were created by testing the lethality and lung damage of the blast waves on 2097 animals from 13 different species. Three models were derived based the orientation of the person with respect to the blast wave. The animals were exposed to one reflecting surface (i.e. a wall or the ground). The blast waves were generated either by detonation or shock tubes. Bowen created injury lethality model for a person in an open field, near a wall, as well as a person in the prone position. The same model is used for all three scenarios (i.e. near-wall, free-field and prone), but a different pressure dose value is used in each case to amplify the pressure as necessary (Figure 4). In all three the curves the incident pressure is required to predict the lethality (Figure 4). The lethality was based on the death rate of the animals within the proceeding 24 hours after blast exposure [8, 10].

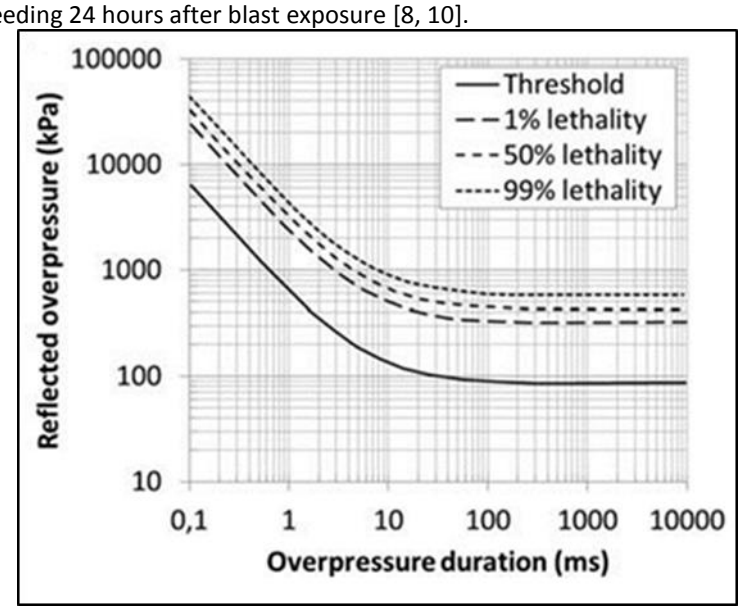

Fig. 4. One of Bowen's lethality curves for a person exposed to a flat rigid reflecting surface [6]

The Bowen model were updated with more data in 2008 by Bass et al. [6] for short duration blasts (30 ms or less) and in 2010 by Rafaels et al. [7] for long duration blasts (10 ms or more). The data set was increased to include over 2500 large animals in more than 50 different experiments. The Bowen curves [10] were compared for both the incident and reflected pressure conditions. The results were similar to Bowen; however, the shape of the longer duration curves differed from those in the short duration study as illustrated in Figure 5. For the longest duration, the curves from

Rafaels et al [7] also differed from the Bowen study by trending downwards. These curves also represented 50% lethality opposed to the 100% lethality of Bowen [6, 7].

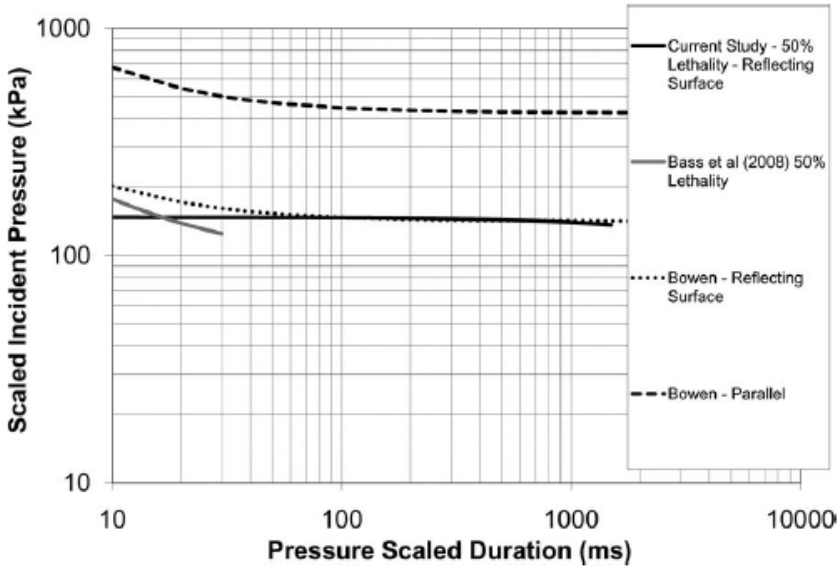

Fig. 5. Comparison of lethality curves from Rafaels [8], Bowen [11] and Bass [7]

Although the models of Bass [6], Rafeals [7], and Bowen [10] are lethality predictors for simple blast waves, a different approach is required for complex blast waves. Complex blast waves typically include many blast waves that may be superimposed on a slow rising pressure. The Axelsson model was developed specifically to address the problems from the other models [9]. The Axelsson model is a simplified single chamber, one-lung mathematical model of the thorax, originating from an older, more complex model developed by Bowen [10] and Fletcher [11]. Axelsson's model is based on experiments performed by Johnson [12].

Johnson's experiments [12] compared the effect of complex blast loading on 255 sheep to the blast wave pressure measured using an instrumented cylindrical blast test device (BTD). The BTD was manufactured from aluminium and instrumented with four pressure gauges at 90˚ intervals along the circumference of the cylindrical structure at a fixed height. Therefore, when used in a test setup, the BTD measures the blast loading from four directions [8].

Axelsson's model used these measured pressures to calculate the response of the chest wall (in terms of displacement, velocity and acceleration) as well as the intrathoracic (i.e. lung) pressure for both complex and simple blast waves profiles [8, 9]. The input of the model was obtained from the blast loading on the BTD cylinder, namely the external reflected overpressure. It is used to measure severity of chest injury to the Adjusted Injury of Severity Index (AISI).

For the more general case, where the body is not parallel to the direction of the incoming blast wave, Axelsson proposed the Chest Wall Velocity Predictor (CWVP) parameter. The maximum and average chest wall velocities are calculated based on the measurements of the four pressure gauges, on the circumference of the BTD, and are then used to determine the severity of the injury according to the AISI [8, 9, 12].

Although Axelsson's model is currently the only specific injury criterion in NATO standard for the prediction of primary blast injuries, its limitation is that it must be coupled with experimental techniques. Furthermore, the type of experimental techniques used by Axelsson cannot directly be implemented on vehicle occupants without some prior modification. Additionally, it should be noted that Axelsson's model is also only a severity predictor and does not predict the risk of injury. It is also unclear if the Axelsson's model is valid for positive-phase durations of less than 0.4 ms as the data set used for validation only includes pressure profiles with positive-phase durations greater than 0.4 ms [8].

The final development in terms of primary blast injury criteria, is Stuhmiller's model. Stuhmiller developed a model which also predicts the incidence and severity of injury in the lungs of mammals in both the free-field and complex environments. The model assumes the mediator of injury to be the compression wave within the lung and thus predicts its intensity. The model greatly simplifies the geometry of the lung and thorax and calculates the irreversible work done by the blast loading on the lungs using a mathematical single degree of freedom model (like Axelsson) and the pressures measured using the BTD [13].

Terrorist actions poses new threats making explosions in urban areas, and thus complex blast related injuries to internal gas containing organs, much more relevant [14]. To study the severity of these injuries, several models have been developed in the past for both simple free-field blasts (Bowen [10] and Bass [6]), as well as complex blast (Axelsson [9] and Stuhmiller [13]). The models of Axelsson and Stumiller are based on measurements taken from a BTD.

The use of explosives by terrorist groups pose greater risk to the soldiers as well as civilians. The rapid release of energy due to an explosion results in an almost instantaneous rise in pressure. As this pressure wave moves outwards from the source of explosion it may cause blast injuries to nearby persons as illustrated in Figure 6. There are three general classifications of blast injury from explosions:

1. Primary injury is caused by the blast wave and encompasses injury to air – containing organs such lung, ear etc.
2. Secondary injury is caused by the impact of fragments from the explosive device or from other debris generated and propelled by the explosion.
3. Tertiary injury results from the displacement – either avulsion of limbs subsequent to fracture by a shock wave or injuries resulting from displacement of the body as a whole.

The most notable primary blast injury is blast lung, which is a contusion of lungs in which blood contaminates the alveoli leading to death. The incidence of primary blast injury is greater in confined spaces because of the increase in the effective loading to the body due to blast reflections which makes blast weapons particularly dangerous in built up areas.

The aim was to validate the BTD by comparison to results from similar tests, where good correlation infers the validity of the device.

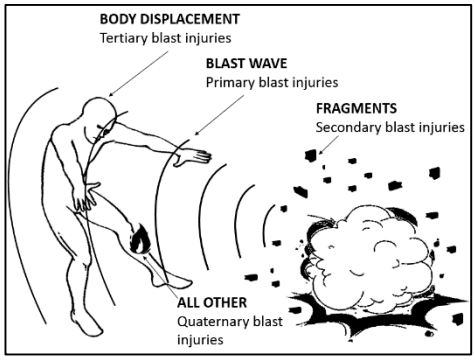

Fig. 6. Damage mechanisms of primary, secondary, tertiary and quaternary blast injuries [1]

A computational model of a Blast Test Device (BTD) was developed to study the complex blast wave-structure interaction. The BTD is a cylindrically-shaped human torso surrogate device instrumented with four pressure sensors used to capture three dimensional (3D) complex blast loading. Experimental BTD results were compared to similar test results published by the French-German Research Institute of Saint-Louis (ISL) and Strasbourg University in France [15-17]. The data were also used to validate the numerical results. The purpose of this study was to develop an assessment method for measuring the blast wave, which may lead to future research in the understanding of primary blast injuries and ultimately, the improvement of protective equipment, to reduce the severity of blast related injuries.

2. Materials and Methods

2.1. Design and Manufacturing of BTD

Various personal vulnerability rigs, or BTD's, are being used internationally for the measurement of human vulnerability to the blast wave pressure. Some of the rigs include, but are not limited to the AUSman – Australia [18], Thoracic rig - United Kingdom [18], GelMan [18] and BTD - United States [9] and Mannequin for the Assessment of Blast Incapacitation and Lethality (MABIL) - Defence Research and Development Canada (DRDC) Valcartier in Canada [19].

A BTD was designed and manufactured for injury assessment from blast overpressure effects and to establish a database for comparison of different injury assessment methods and to investigate various protection solutions. A simple cylindrical shape was chosen for the initial design to allow for the validation of results by comparison to similar studies [12, 15-17].

The BTD comprises of a high-density polyethylene (HDPE) cylinder with an outer diameter of 300 mm, height of 762 mm and wall thickness of 20 mm (Figure 7). The top and bottom of the cylinder are sealed using 20 mm thick lids, making the total height 802mm. The lids are secured using bolts after closure. An access hole is located on the side of the cylinder, just above the bottom lid, for easy access to the internal *DTS TDAS Slice Nano* (Diversified Technical Solutions, Seal Beach, CA) data acquisition system at a sample rate of 500 kHz. The cylinder is mounted on a steel stand, with a height of 479 mm.

The BTD has eight interchangeable polyoxymethylene mounting positions for pressure gauges around the circumference but only four sensors were used during the current study (Figure 7). The fittings are mounted flush with the surface of the cylinder. The mountings are positioned at the cylinder's half height, which is at a height of 880 mm above the ground. The mountings isolate the sensors mechanically and electronically to avoid drift, electromagnetic effects and interferences. Thermal protection is used to insulate the pressure sensors from flash temperatures as a result of the blast.

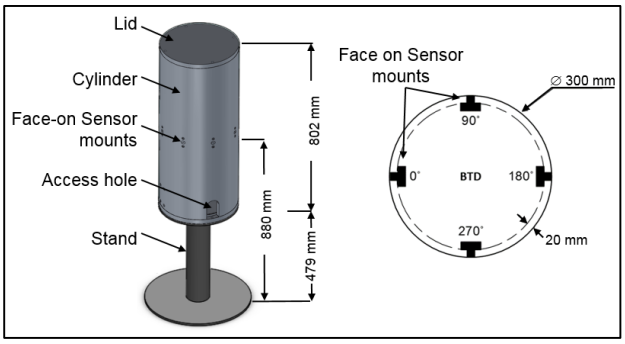

Fig. 7. The BTD

2.2. Pressure Gauge Selection

To cover a range of pressure measurements, two various ranges of the piezoresistive *Endevco* 8530 transducer series [20] were selected for the use in the BTD; namely 100 psi and 200 psi. The *Endevco* 8530 series was chosen because they are typically less susceptible to noise and can measure the incident wave profile accurately.

The orientation of the pressure sensor with regard to the pressure wave is important as it determines which pressure is measured. Face-on pressure sensors measure the reflected pressure wave, which is the pressure that develops if a blast wave strikes an infinitely large wall. The sensing element of face-on sensors is parallel to the direction of blast wave propagation and measures the static and the dynamic pressure (i.e. total pressure) as shown in Figure 7. The dynamic pressure is the force associated with the blast wind (the movement of air particles at the leading edge of the shock wave). Side-on pressure gauges measure the static pressure, also known as the incident pressure [21] and perpendicular to the direction of blast wave propagation, as shown in Figure 8.

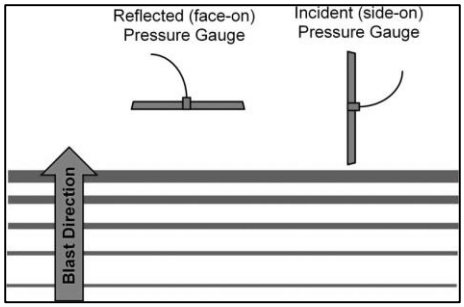

Fig. 8. Face-on versus side-on pressure gauges [21]

3. Experimental Analysis

3.1. Experimental Setup

Blast tests conducted by Boutillier et al. [16] using their in-house developed and manufactured BTD were compared to the test conducted with The BTD torso surrogate. The difference between the two sets of tests was the explosive

material that was used. Composition-4 (C-4) was used by Boutillier et al. [16] and Plastic Explosive No. 4 (PE4) was used during the tests described in this paper. C-4 and PE4 are very similar in composition and produce comparable results in terms of pressure and impulse [22]. The experimental results from the two sets of tests were compared with respect to peak incident pressures, peak reflected pressures and positive phase duration from the measured signals.

The tests involved detonating a small, free-in-air spherical charge over a flat concrete surface at a distance of 2 m from the BTD. The detonator was inserted into the top of the charge. The 0.3 kg charge was positioned at three different heights, referred to as the height of burst (HoB); namely 220 mm, 440 mm and 880 mm measured from the ground to the bottom of the spherical charge. These heights were selected by Boutillier et al., as described in [16], with the aim of subjecting the BTD to various pressure loadings, which were deemed representative of the loadings typically incurred by soldiers or armed forces in the field. The heights refer to a charge detonating close to the ground, an intermediate charge height and a height corresponding to the mid-sternum height of a human respectively. Depending on the charge height and size, pressure profiles ranging from simple to complex are generated. A total of 9 tests, as summarised in Table 1, were performed.

Table 1. Experimental parameters

Test series	HoB [mm]	Explosive material	Charge mass [kg]	Charge radius [mm]	Number of test repetitions
1	220	PE4	0.3	36	4
2	440	PE4	0.3	36	3
3	880	PE4	0.3	36	2

The typical experimental setup is shown in Figure 9 and schematically in Figure 10. Three additional side-on pressure sensors were used to measure the incident blast wave pressure at 90˚ at a standoff distance of 2 m. The sensors are labelled according to their angular position around the threat, as indicated. The side-on pencil probe sensors were mounted on stands at a height of 880 mm, pointing radially inwards and angled towards the centre of the charge for all HoB configurations.

Due to the symmetrical nature of the setup, all the side-on sensors should measure the same pressure. Sandbags were used to provide a suitable fixation for accurate alignment and support of the pencil probes.

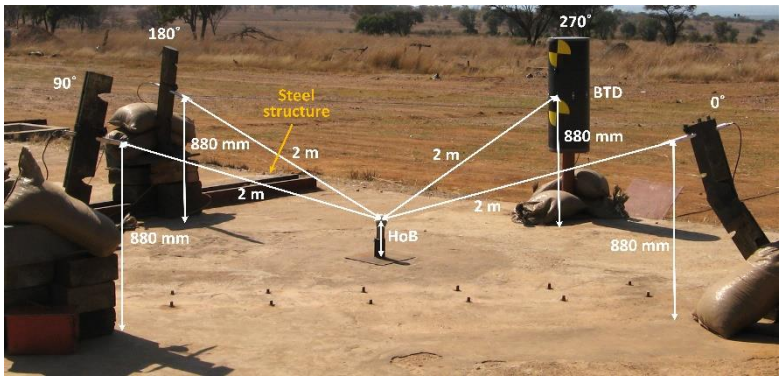

Fig.9. Photograph of the experimental setup

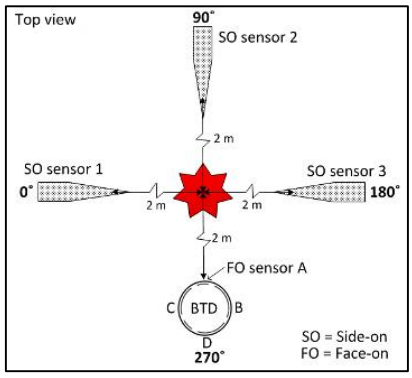

Fig. 10. Schematic of the experimental setup

Two high speed cameras were used to record the experiments in real time. The video footage was analysed subsequent to the tests to monitor the propagation of the blast wave, as well as to determine the triple point of the blast wave.

3.2. Experimental Results

The temporal pressure profiles are plotted in Figure 9 for each HoB configuration. A large steel barrier located on the ground close to the 180˚ side-on sensor compromised the pressure measurement of the 180˚ sensor by creating a more complex pressure profile due to blast wave reflections. Therefore, the results from the 180˚ side-on sensor were discarded from the analysis. The steel structure can be seen in Figure 11. The average pressure measurement of both

the 0˚ and 90˚ side-on sensors for all test repetitions is plotted on a single graph. The average pressure measurement of the front BTD face-on sensor for all test repetitions is plotted. The standard deviation of the test results is also indicated (± σ bounds). The results of the B, C and D BTD sensors are not presented.

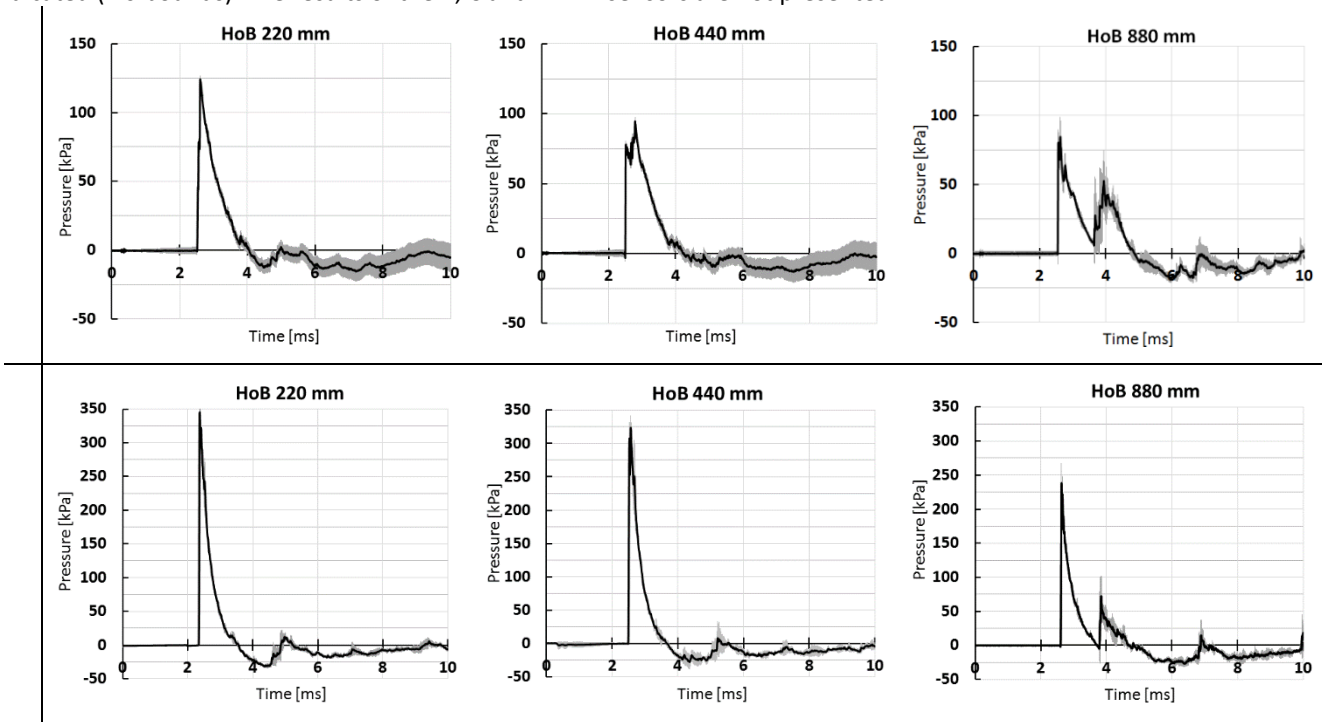

Fig. 11. Average experimental results

For the 220 mm HoB configuration, the pressure profile has the characteristic Friedlander form with a single peak overpressure. Because only one blast wave was recorded, it can be accepted that this was the Mach wave (i.e. the sensors were below the triple point). The peak incident overpressure is 124.2 ± 0.95 kPa and the peak reflected overpressure is 345.3 ± 71.8 kPa.

For the 440 mm HoB configuration, a blast wave with an incident pressure peak of 94.6 ± 10.3 kPa was measured. A peak reflected pressure of 323.8 ± 72.1 kPa was measured at the front of the BTD. This HoB configuration is midway between the other two configurations; therefore, it was expected that the sensors will be on or close to the triple point trajectory. A pressure profile between the ideal simple and complex waveforms was expected. This type of pressure profile was recorded by the side-on pressure sensors. However, the face-on pressure sensor recorded a simple blast wave.

For the 880 mm HoB configuration, the pressure profile displays the traits of a typical complex blast wave with two distinct peaks. The first peak represents the initial incident blast wave and the second peak represents the reflected blast wave. It can be accepted that the sensors were above the triple point. The side-on and face-on pressures of the first peak are 84.5 ± 10.6 kPa and 238.1 ± 63.4 kPa respectively. As the HoB increased from 220 mm to 880 mm, the intensity of the incident overpressure of the blast wave decreased by 32%.

All the results, except the face-on sensor in the 440 mm HoB configuration, show good correlation in terms of the form of the blast wave, rise time and positive phase duration. The peak pressures also compare well, however, there is a notable difference in the intensity of the reflected pressure peak in the 880 mm HoB configuration. Boutillier et al. [16] measured a stronger reflected blast wave. This could be attributed to differences in surface conditions. Differences also exist in the arrival time of the blast wave for some cases, which could be due to sensor misalignment or differences/errors in sensor positioning. The only experimental result that does not compare well to the published result is the face-on sensor in the 440 mm HoB configuration. This could be due to differences in the reflective surface that was used between the two experiments. Boutillier et al. [16] recorded a blast wave with a shape that is expected, that is somewhere between simple and complex (i.e. close to the triple point). In this study, a simple waveform was measured, indicating that the sensor was below the triple point in the Mach regime.

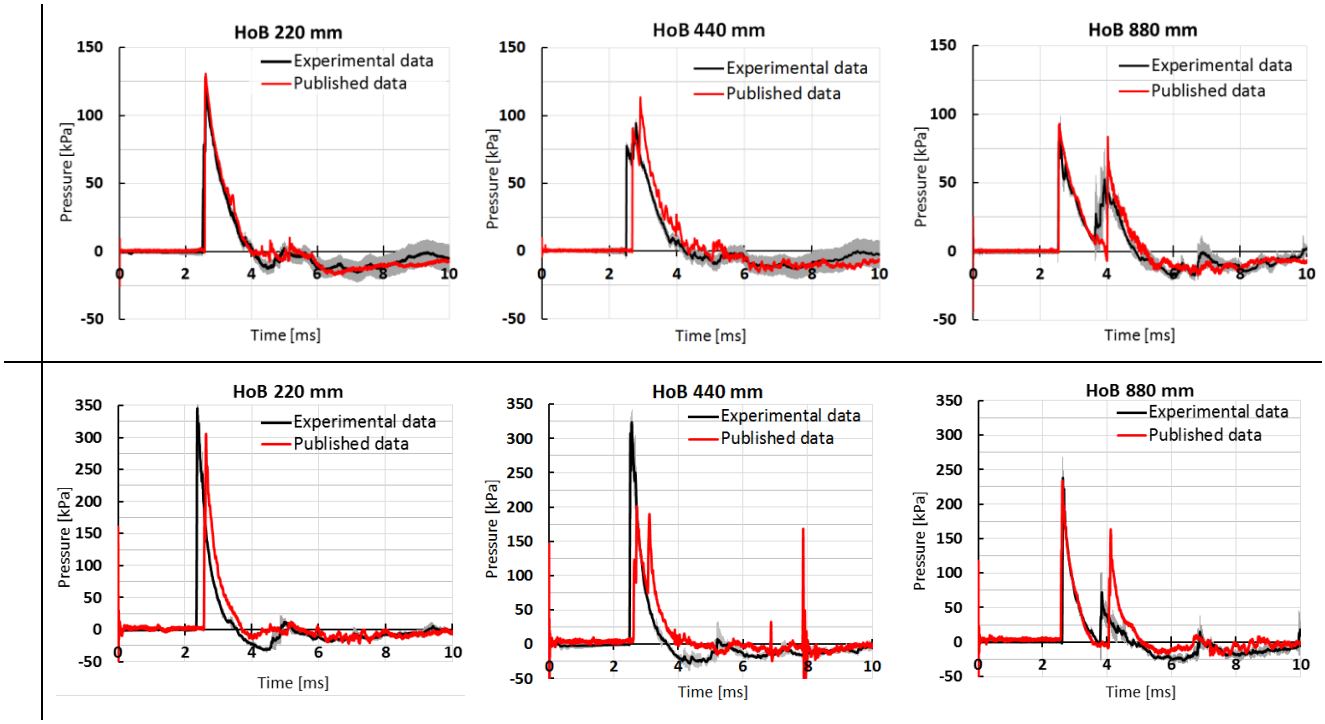

Fig. 11. Comparison of experimental data to published data

The results obtained depend on various factors in the experimental setup, such as the type of sensor used, sensor mounting method, thermal sensitivity of the sensors, BTD construction, data acquisition sampling rate, signal conditioning and filtering, BTD orientation to the blast loading etc. as well as ground shocks, ambient conditions and surrounding structures.

4. Numerical Simulation

4.1. Computational Model

The computational analysis was conducted with the use of *MSC Dytran*. A half-symmetry 3D model, shown in Figure 12, was created to simulate the experiments. Each HoB configuration was modelled.

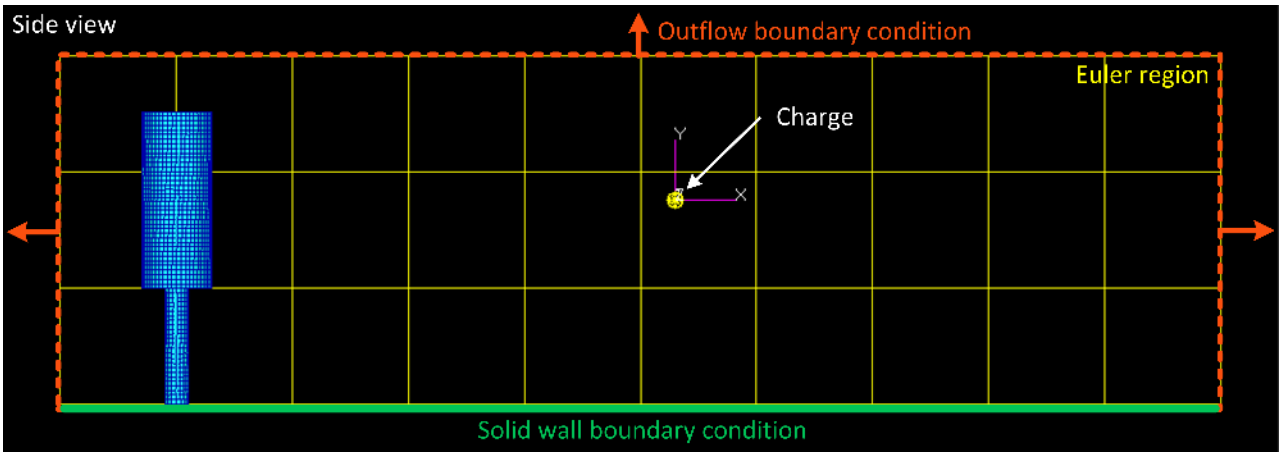

Fig. 12. BTD 3D computational model for the 880 mm HoB configuration

The simulation was divided into steps:

- A simulation of the explosion in the very first moments was realized. The physical detonation of the blast was not modelled; instead the charge was modelled as a sphere of air with the same dimensions as the explosive compressed to the density of PE4 with similar internal energy. This represents the blast event just moments

after detonation. As soon as the simulation starts, the region of compressed air expands rapidly. The simulation is axisymmetric around the Z axis as only the charge and the surrounding air are modeled. The objective was to accurately model the first moments of the scenario. The simulation was performed until 40µs after detonation.

- The results of the first simulation were mapped into a larger domain, which also axisymmetric and pursues the propagation of the blast after the 40µs until 2.1ms, i.e. before it first hits the target. Then 3D blast/target interaction is modeled in a 3D domain. The results of the second simulation were mapped into this 3D simulation, where the target is modeled. The simulation was carried from 2.1 ms until 10ms to correspond with the measured data.
- Linear quadrilateral elements were used to model the solid structure (i.e. the BTD and stand), which was solved using the Lagrangian solver.

Only the BTD was modelled, the additional side-on pressure sensors and their stands were not modelled. The Eulerian mesh was modelled with approximately 106 hexagonal elements and it was geometrically graded to refine the mesh in regions of interest; around the blast and pressure measurement points. The dimensions and mesh sizes were chosen to reproduce as accurately as possible the blast and its interaction with the target while maintaining a manageable computational cost. Coupling surfaces were used to define fluid-structure interaction between the air and the BTD. Soil was not included in the model; the ground surface was represented as a solid wall (i.e. an ideal reflective boundary). Details of the material models and parameter sets are listed in Table 2.

Table 2. Parameter sets and material models

Component	Material	Equation of state
Air	Air	Ideal gas
BTD cylindrical body	Rigid (with a representative density)	N/A
BTD stand	Rigid (with a representative density)	N/A

4.2. Computational Results

The typical results of the blast wave developed in the 440 mm HoB configuration for the first 1.5 ms are shown in Figure 13. The incident wave, followed by the reflected wave, can be observed. The pressure decreases as the blast wave propagates away from the centre of blast. The longer wave propagation is shown in Figure 14.The comparison of all the results for all configurations are shown in Figure 14. As the HoB varies, the height of the initial fluid–structure interaction aslo varies.

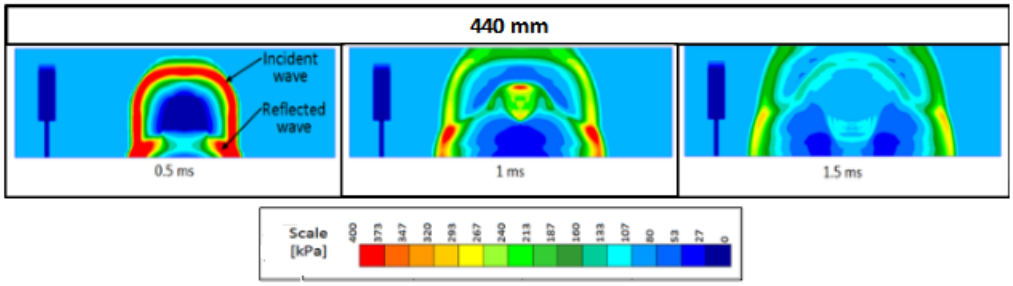

Fig. 13. A time sequence of the blast event showing the typical blast wave development for the 440 mm HoB configuration with legend at the bottom

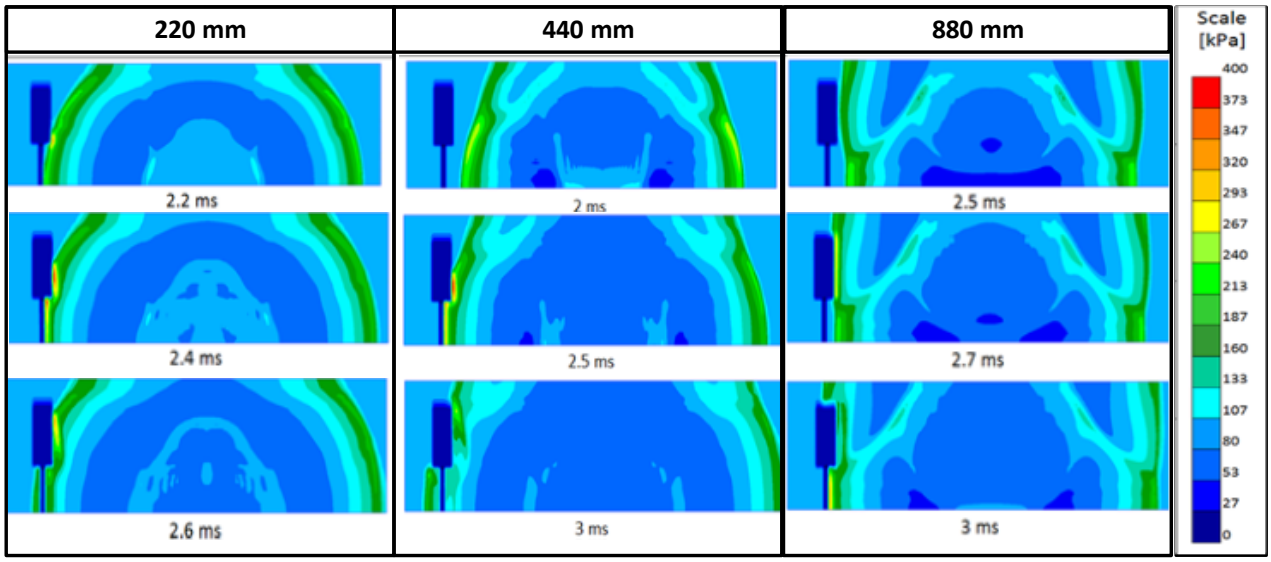

Fig. 14. Fluid-structure interaction for the 220 mm, 440 mm and 880 mm configurations

The pressure profiles at the location of the BTD's front face-on sensor and the additional side-on pressure sensors were plotted and compared to the pressure profiles obtained experimentally. The results are shown in Figure 15.

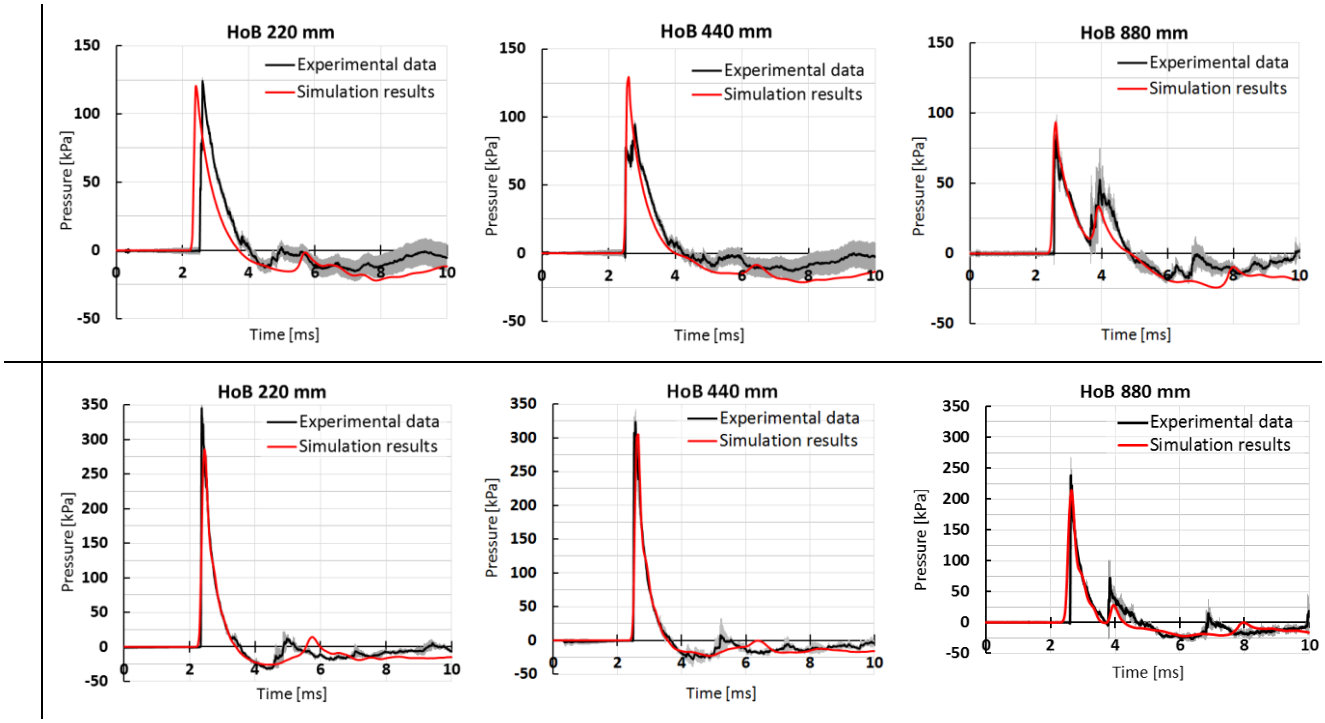

Fig. 15. Comparison of the simulation results to the experimental data

All the results show good correlation in terms of the form of the blast wave, rise time and positive phase duration. There are some differences in terms of the peak pressures, most notably the side-on pressure in the 440 mm HoB configuration, the face-on pressure in the 220 mm configuration and the peak pressure of the reflected blast wave in the 880 mm HoB configuration. In the 440 mm configuration, the simulation results indicate that the sensor is in the Mach regime, which can also be observed in Figure 13. For the 220 mm configuration, the peak face-on pressure is comparable to the published results. Differences also exist in the negative phase.

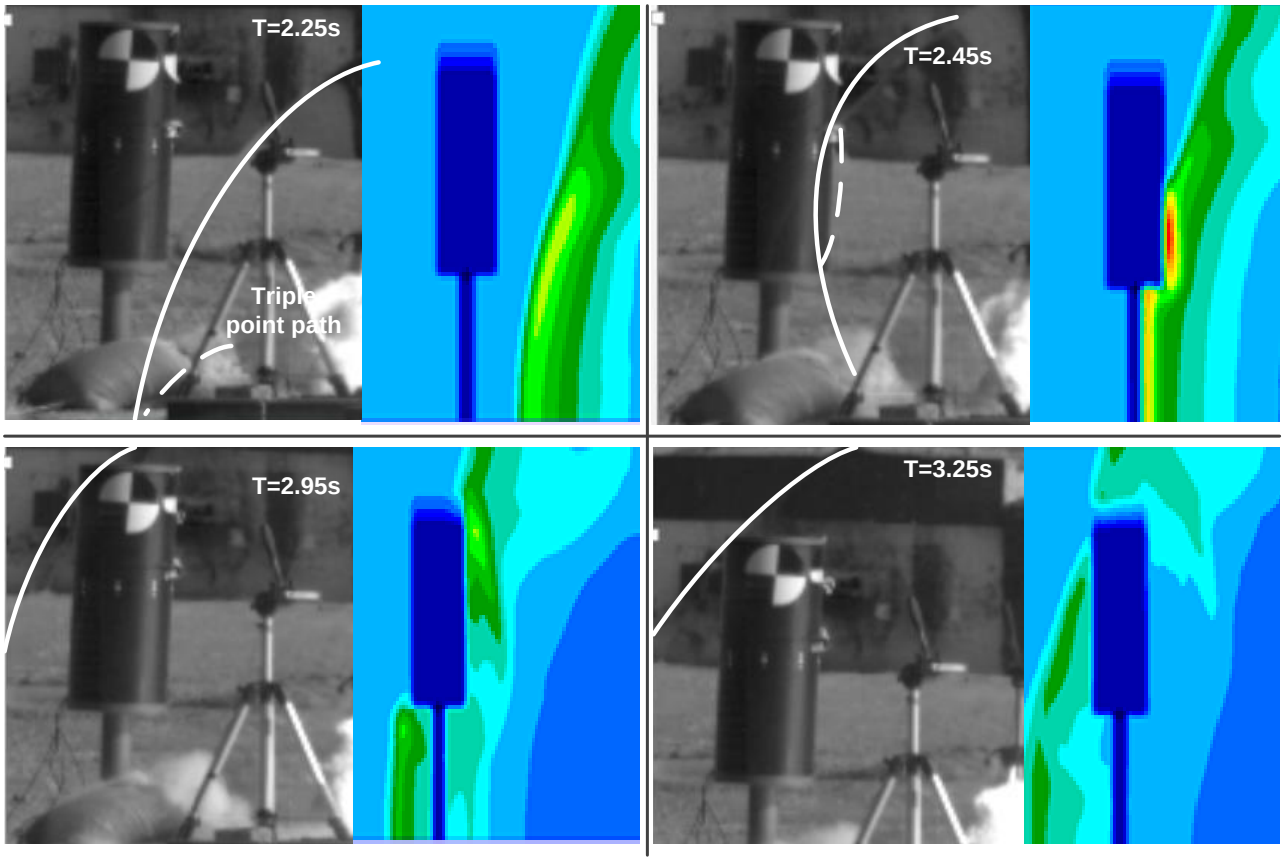

Fig. 16. Comparison of the experimental and simulated blast wave propagation

The experimental blast wave propagation obtained from high speed video footage is compared to the simulated blast wave propagation for the 440 mm HoB configuration in Figure 16. The time frames show evidence of accurate reproduction of the shock behaviour:

- At t = 2.25 ms: The blast wave has not reached the BTD yet. The target (i.e. BTD sensor) is on the triple point path. The characteristics of the blast (Mach stem, incident and reflected shock) are reproduced numerically.
- At t = 2.45 ms: The blast wave reaches and interacts with the target.
- At t = 2.95 ms: The front reflections expand and produce a pattern identical to the numerical one. The shock wave diffracts at the top of the cylinder and reflects at the bottom. The shock wave below the cylinder diffracts. This diffraction and the other patterns are reproduced numerically.
- At t = 3.25 ms: The shockwave propagating above the cylinder diffracts. The other waves pursue their propagation.

5. Discussion

The use of explosives by terrorists, or during armed conflict, remains a major global threat. Increasingly, these events occur in the civilian domain, and can potentially lead to injury and loss of life, on a very large scale. The blast phenomenon is mainly characterised by its scale of very short time, in which the simplest pressure profile can be described with the Friedlander waveform. This profile gains in complexity as reflections are added (ground, wall, or obstacle). In few microseconds, the biological structures are damaged by the shock-wave. One of the research aims is to develop and evaluate technologies and solutions to mitigate the blast threat on soldiers. Therefore, it is important to develop an understanding of the blast-body interaction. A simplified rigid torso surrogate, referred to as the BTD was designed and locally manufactured. The BTD was investigated experimentally and numerically.

In general, for all three configurations, there was good correlation between the experimental and simulated results. For example, the classical Friedlander waveform as measured by the front and side sensors are well reproduced for all the configurations despite the complex phenomena. It can be concluded that phenomena such as diffraction, rarefaction, Mach reflection on the ground etc. are well reproduced numerically.

The experimental and published results compare well in terms of waveform, rise and decay times and positive phase duration. There are some differences in peak pressure values, which can be attributed to differences and/or impurities

in the explosive materials and differences in ground reflected shocks. This will have to be investigated further by conducting additional tests.

6. Conclusion

In the aim of mitigating the blast threat of the dismounted soldier, an important step is the understanding of the blast/body interaction. A rigid human torso surrogate, referred to as a blast test device, has been manufactured locally. The BTD is a tool that can be used for predicting the severity of thoracic injuries and therefore forms a valuable part of protection research. It can be used to evaluate various protection methodologies, to characterise blast waves and contribute to the development of injury criteria. The characterisation of complex blast waves is of particular interest due to the increasing prevalence of urban warfare.

A rudimentary computational model of the blast test device in an open field was created and validated using the experimental data. With the confidence on the accuracy of the model, supported by a comparison with high-speed videos, the shock wave behavior was studied numerically. The full blast interaction with the BTD torso surrogate was exhaustively described. This model can be used to support future blast wave-structure interaction research.

Acknowledgements

The authors would like to acknowledge the sponsor of this project, Armscor, as well as the staff at the CSIR's Detonics, Ballistics and Explosives Laboratory (DBEL), the CSIR Landward Sciences (LS) Protection and Survivability research group, especially M.E. Mokalane, as well as the CSIR LS mechanical workshop staff for their assistance and support. Dr J Boutillier from Strasbourg University in France for providing us with their experimental data.

References

[1] Cooper GJ. (1996). Protection of the Lung from Blast Overpressure by Thoracic Stress Wave Decouplers. Journal of Trauma, 40(3):105–110.

[2] Belmont PJ, Schoenfeld AJ, Goodman G. (2010) Epidemiology of Combat Wounds in Operation Iraqi Freedom: Orthopaedic Burden of Disease. Journal of Surgical Orthopaedic Advances.

[3] Johnson DL, Yelverton JT, Hicks W, Doyal R. (1993) Blast Overpressure Studies with Animals and Man: Biological Response to Complex Blast Waves. Final Report, US Army Medical Research and Development Command

[4] Gupta RK, Przekwas A (2013). Mathematical models of blast-induced TBI: current status, challenges, and prospects. Frontiers in neurology, 4, p.59.

[5] Jiang Z, Takayama K, Moosad KPB, Onodera O, Sun M 1998. Numerical and experimental study of a micro-blast wave generated by pulsed-laser beam focusing. Shock Waves, Springer Verlag, 8. Pp. 337-349.

[6] Bass CR, Rafaels KA, Salzar RS (2008). Pulmonary injury risk assessment for short-duration blasts. Journal of Trauma and Acute Care Surgery, 65(3), p.604-615.

[7] Rafaels KA, Cameron R, Panzer MB, Salzar RS (2010). Pulmonary injury risk assessment for long-duration blasts: a meta-analysis. Journal of Trauma and Acute Care Surgery, 69(2), p.368-374.

[8] NATO (2007). Test Methodology for Protection of Vehicle Occupants against Anti-Vehicular Landmine Effects. NATO, RTO, Research and Technology Organization, TR-HFM-090. Neuilly-sur-Seine Cedex: RTO/NATO. URL: http://www.dtic.mil/dtic/tr/fulltext/u2/a473218.pdf accessed 9 May 2018.

[9] Axelsson H, Yelverton JT (1996). Chest wall velocity as a predictor of nonauditory blast injury in a complex wave environment. Journal of Trauma and Acute Care Surgery, 40(3S), p.31S-37S.

[10] Bowen IG, Fletcher ER, Richmond DR (1968). Estimate of man's tolerance to the direct effects of air blast. Lovelace foundation for medical education and research, Albuquerque NM.

[11] Fletcher ER (1971). A model to simulate thoracic responses to air blast and to impact (No. AMRL-TR-71-29-paper-1). Lovelace foundation for medical education and research, Albuquerque AM.

[12] Johnson DL, Yelverton JT, Hicks W, Doyal, R (1993). Blast overpressure studies with animals and man: Biological response to complex blast waves. EG AND G INC ALBUQUERQUE NM.

[13] Stuhmiller JH, Ho KHH, Vander Vorst MJ, Dodd KT, Fitzpatrick T, Mayorga M (1996). A model of blast overpressure injury to the lung. Journal of biomechanics, 29(2), p.227-234.

[14] Teland JA, Van Doormaal JCAM (2012). Blast wave injury prediction models for complex scenarios. Proc 22nd MABS-Military Aspects Blast and Shock. Bourges, France, Paper, 87, p.4-9.

[15] Boutillier J, De Mezzo S, Deck C, Ehrhardt L, Magnan P, Naz P, Willinger R (2016). Shock-wave interaction with reduced-scale simplified torso surrogates. In IRCOBI Conference Proceedings.

[16] Boutillier J, De Mezzo S, Deck C, Ehrhardt L, Magnan P, Naz P, Willinger R (2016). New experimental data on blast interaction with instrumented structures. In Military Aspects of Blast and Shock Symposium MABS24. Halifax, Canada.

[17] Ehrhardt L, Boutillier J, Magnan P, Deck C, De Mezzo S, Willinger R, Naz P. Numerical simulation of the air blast interaction with simplified structures.

[18] Murray SB, Anderson CJ, Gerrard KB, Smithson T, Williams K, Ritzel DV (2009). Overview of the 2005 Northern Lights Trials. In Shock Waves (pp. 335-340). Springer, Berlin, Heidelberg

[19] Ouellet, S., Williams, K. Characterisation of Defence Research and Development Canada's Mannequin for the Assessment of Blast Incapacitation and Lethality (DRDC MABIL). Proceeding of PASS conference, 2008, Brussels.

[20] Meggitt Pressure transducers. URL: https://buy.endevco.com/pressure.html? applications & industry= 533&range_full_scale_psi=769_770& reference_type=783 accessed 9 May 2018.

[21] Boutillier J, Deck C, Magnan P, Naz P, Willinger R. A critical literature review on primary blast thorax injury and their outcomes. Journal of Trauma and Acute Care Surgery, 2016 Aug 1;81(2):371-9.

[22] Bogosian, D, Yokota, M and Rigby, SE (2016). TNT equivalence of C-4 and PE4: a review of traditional sources and recent data, 24th Military Aspects of Blast and Shock MABS24.